

**NASA-CR-195808**

Design of a ZVS PWM Inverter for a Brushless DC Motor in an EMA Application

J. Brett Bell, R. M. Nelms\*, and Michael T. Shepherd

Department of Electrical Engineering

Auburn University, AL 36849

Phone: (205) 844-1830

FAX: (205) 844-1809

*11-39-12  
26403*

\* - corresponding author

Topical area: brushless dc motor control

ABSTRACT

The Component Development Division of the Propulsion Laboratory at Marshall Space Flight Center (MSFC) is currently investigating the use of electromechanical actuators for use in space transportation applications such as Thrust Vector Control (TVC). These high power servomechanisms will require rugged, reliable, and compact power electronic modules capable of modulating several hundred amperes of current at up to 270 Vdc. This paper will discuss the design and implementation of a zero-voltage-switched PWM inverter which operates from a 270 Vdc source at currents up to 100 A.

(NASA-CR-195808) DESIGN OF A ZVS  
PWM INVERTER FOR A BRUSHLESS DC  
MOTOR IN AN EMA APPLICATION  
(Auburn Univ.) 8 p

N95-12620

Unclas

G3/39 0026403

## Design of a ZVS PWM Inverter for a Brushless DC Motor in an EMA Application

The Component Development Division of the Propulsion Laboratory at Marshall Space Flight Center (MSFC) is currently investigating a class of Electromechanical Actuators (EMAs) for use in space transportation applications such as Thrust Vector Control (TVC) and Propellant Control Valves (PCV). These high power servomechanisms will require rugged, reliable, and compact power electronic modules capable of modulating several hundred amperes of current at up to 270 volts. MSFC has selected the brushless dc motor for implementation in EMAs.

This paper will describe the design and implementation of a zero-voltage-switched PWM inverter for the MSFC actuator testbed. For the present experiments, the inverter must be rated for a maximum current of 100 A. Because of this high current level, zero-voltage switching characteristics are desirable to reduce switching stresses, switching losses, and EMI. The ZVS inverter [1-3] selected for implementation is shown in Figure 1. As can be seen in this figure, a waveshaping circuit has been added to a conventional three-phase inverter. The function of this waveshaping circuit is to shape the input voltage to the three-phase inverter such that it is zero for a short period of time. During this zero voltage period, any of the semiconductor switches in the three-phase inverter may be turned on or off. Switch  $S_r$  is redundant since its function can be accomplished by the simultaneous conduction of two switches in any one leg of the inverter.

The operation of the waveshaping circuit and inverter will now be described assuming that all components are ideal. Beginning with switches  $S_1$  and  $S_2$  closed and switches  $S_3$  and  $S_r$  open, the inverter is in steady-state with one of the top switches ( $T_1$ ) and one of the bottom switches ( $T_5$ ) conducting. A command is received from the inverter controller to change the status of an inverter switch. At this point, switch  $S_3$  is closed and current begins to increase linearly in the inductor. Once sufficient energy has been stored in the inductor, switch  $S_1$  is turned off at zero voltage disconnecting the source from the inverter, which is necessary so that the inverter input voltage will ring down to zero. After  $S_1$  is opened, the energy stored in the inductor begins to discharge capacitors  $C_1$  and  $C_2$ . When voltages  $v_{C1}$  and  $v_{C2}$  reach zero,  $S_2$  is turned off at zero voltage while  $S_r$  is turned on at zero voltage shorting the inverter input. The inverter switches are changed during this zero voltage period. The inductor current is positive at the beginning of this time interval and is negative at the end. Voltage  $v_{C1}$  actually goes negative during this time interval and returns to zero at which time the status of both  $S_2$  and  $S_r$  are changed at zero voltage. Voltages  $v_{C1}$  and  $v_{C2}$  begin to increase positively. When they reach  $V_s$ , the diode in anti-parallel with  $S_1$  begins to conduct so that  $S_1$  can now be turned on at zero voltage

reconnecting the source to the inverter. Since the inductor current is negative during the recharge of capacitors  $C_1$  and  $C_2$ , switch  $S_3$  can be turned off at zero voltage because its anti-parallel diode is conducting. The anti-parallel diode of  $S_3$  turns off when the inductor current reaches zero. The waveshaping circuit then waits for the next command from the inverter controller to begin the process of ringing the inverter input voltage to zero.

Figure 2 gives representative waveforms for  $v_{C1}$ ,  $v_{C2}$ , and  $i_L$ . Waveforms from a prototype system which contains a 5 Hp brushless dc motor are shown in Figure 3. The top waveform is  $v_{C2}$ , which is the inverter input voltage. The bus voltage ( $V_s$ ) is approximately 70 V. The inverter input voltage is clamped at zero for about 10  $\mu$ s. The inductor current waveform is the bottom trace in this figure.

The design equations for the circuit of Figure 1 are developed assuming that the inverter can be modeled as a constant current source  $I_0$ , which is always assumed to be positive with respect to the direction shown in Figure 1. These equations are developed in references [1-3] and have been modified here so that many of the quantities are expressed in terms of the inductance  $L$  and the length of the zero voltage interval,  $t_3-t_2$ .

$$\omega_1 = \frac{1}{\sqrt{L(C_1 + C_2)}} \quad \omega_2 = \frac{1}{\sqrt{LC_1}} \quad cratio = \frac{C_2}{C_1} \quad C_1 = \frac{1}{L} \left( \frac{t_3 - t_2}{\pi} \right)^2$$

$$Z_0 = \sqrt{\frac{L}{C_1 + C_2}} = \sqrt{\frac{1}{1 + cratio}} \frac{\pi L}{t_3 - t_2}$$

$$t_1 - t_0 = \frac{L}{V_s} I_p \quad t_2 - t_1 = \frac{1}{\omega_1} \sin^{-1} \left[ \frac{V_s}{V_s + 2Z_0 I_0} \right]$$

$$t_3 - t_2 = \frac{\pi}{\omega_2} \quad t_4 - t_3 = \frac{\pi}{2\omega_1} \quad t_5 - t_4 = \frac{L}{V_s} I_0$$

$$I_{Lmax} = \frac{V_s}{Z_0} + I_0 = V_s \sqrt{1 + cratio} \frac{t_3 - t_2}{\pi L} + I_0$$

$$V_{C1max} = \sqrt{\frac{L}{C_1}} I_{Lmax} = \sqrt{1 + cratio} V_s + \frac{\pi L}{t_3 - t_2} I_0$$

$$I_p = \frac{V_s}{Z_0} \cot[\omega_1(t_2 - t_1)] - I_0$$

Beginning with the input voltage  $V_s$  and the maximum inverter current, the designer may select the inductance  $L$  and the time interval  $t_{32} = (t_3 - t_2)$  and then calculate the additional circuit parameters. For the ZVS inverter on the MSFC testbed,  $V_s = 270$  V and the maximum inverter current  $I_{0\max} = 100$  A. Three other quantities must be selected now:  $L$ ,  $t_{32}$ , and cratio. One of the compromises in the design is to reduce  $V_{C1\max}$  while maintaining a reasonable value for  $I_{L\max}$ . Values of  $V_{C1\max}$  close to  $V_s$  result in very high levels for  $I_{L\max}$ . The value of  $V_{C1\max}$  increases rapidly as  $I_{L\max}$  is reduced. Examination of the expression for  $V_{C1\max}$  indicates that this quantity increases with cratio. As a result, small values of cratio will result in lower values of  $V_{C1\max}$ . Selecting cratio = 0.1,  $L = 5\mu\text{H}$ , and  $t_{32} = 5\mu\text{s}$  yields the following circuit parameters,

$$\begin{aligned}
 C_1 &= 0.50 \mu\text{F} & C_2 &= 0.05 \mu\text{F} & V_{C1\max} &= 597.3 \text{ V} & I_{L\max} &= 190.1 \text{ A} \\
 I_p &= 175.8 \text{ A} & Z_0 &= 3 \Omega & t_1 - t_0 &= 3.26 \mu\text{s} & t_2 - t_1 &= 0.527 \mu\text{s} \\
 & & & & t_4 - t_3 &= 2.62 \mu\text{s} & t_5 - t_4 &= 1.85 \mu\text{s}
 \end{aligned}$$

One drawback from selecting cratio = 0.1 is that  $C_1$  carries about ten times more current than  $C_2$ . For the parameters above, a GE 97F8585 capacitor is used for  $C_1$ , while a Cornell-Dubilier DPPM10S47K polypropylene capacitor is employed for  $C_2$ . The  $5\mu\text{H}$  inductor, which must be designed for high peak currents, is constructed using two Magnetics, Inc. powdered iron cores (Part. No. 58868-A2) epoxied together and nine turns of copper braided conductor.

The control system for the EMA determines the current command for the inverter. The Hall effect signals from the brushless dc motor are decoded to determine which of the switches  $T_1 - T_6$  should be conducting. The motor current is regulated using a hysteresis type control scheme. At any instance of time, only two switches in the inverter are conducting. Of the two switches, the bottom switch is toggled on and off to regulate the current. In most applications, two of the motor phase currents are usually measured, and a signal proportional to the third is created using these two measurements. In this control system, the link current  $I_0$  is measured and used as the input to the current regulator. Since only two switches are conducting at a time, the link current is equal to the motor phase current. When the link current reaches the commanded level, the bottom switch is turned off. The motor phase current begins to decrease while the link current goes to zero. In order to achieve a hysteresis type control, the turn on of the bottom switch is delayed by a certain time interval. The bottom trace of Figure 4 shows the link current in the inverter of

the 5 Hp prototype system under this type of operation. The link current goes to zero when the bottom switch is turned off. This switch remains off for about 10  $\mu$ s before it is turned back on. It conducts until the link current reaches the command level. The inverter input voltage is shown in the top trace. Note that this voltage is reduced to zero by the waveshaping circuit each time the inverter controller commands a current change.

### References

[1] J. He, "Parallel Resonant DC Link Circuit - a Novel Zero-Voltage-Switching Topology with Minimum Voltage Stresses for DC-AC Power Conversion," Ph.D. Dissertation, University of Minnesota, Minneapolis, July, 1990.

[2] J. He and N. Mohan, "Parallel Resonant DC Link Circuit - A Novel Zero-Switching Loss Topology with Minimum Voltage Stresses," IEEE Power Electronics Specialists Conference Record, 1989, pp. 1006-1012.

[3] J. He, N. Mohan, and B. Wold, "Zero-Voltage-Switching PWM Inverter for High-Frequency DC-AC Power Conversion," IEEE Transactions on Industry Applications, Vol. 29, No. 5, September /October 1993, pp. 959-968.

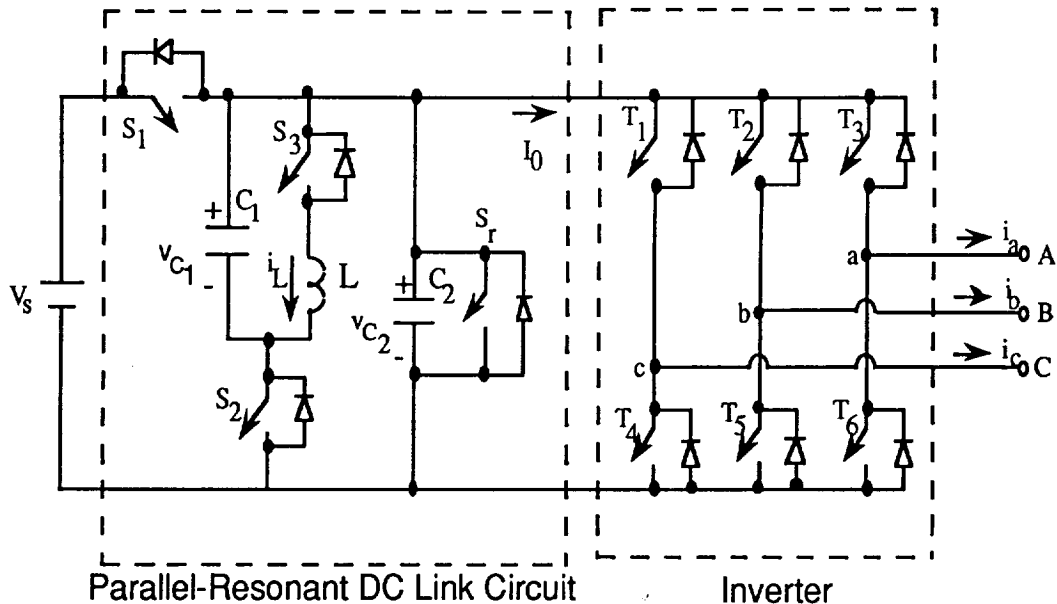


Figure 1. ZVS PWM Inverter [1-3].

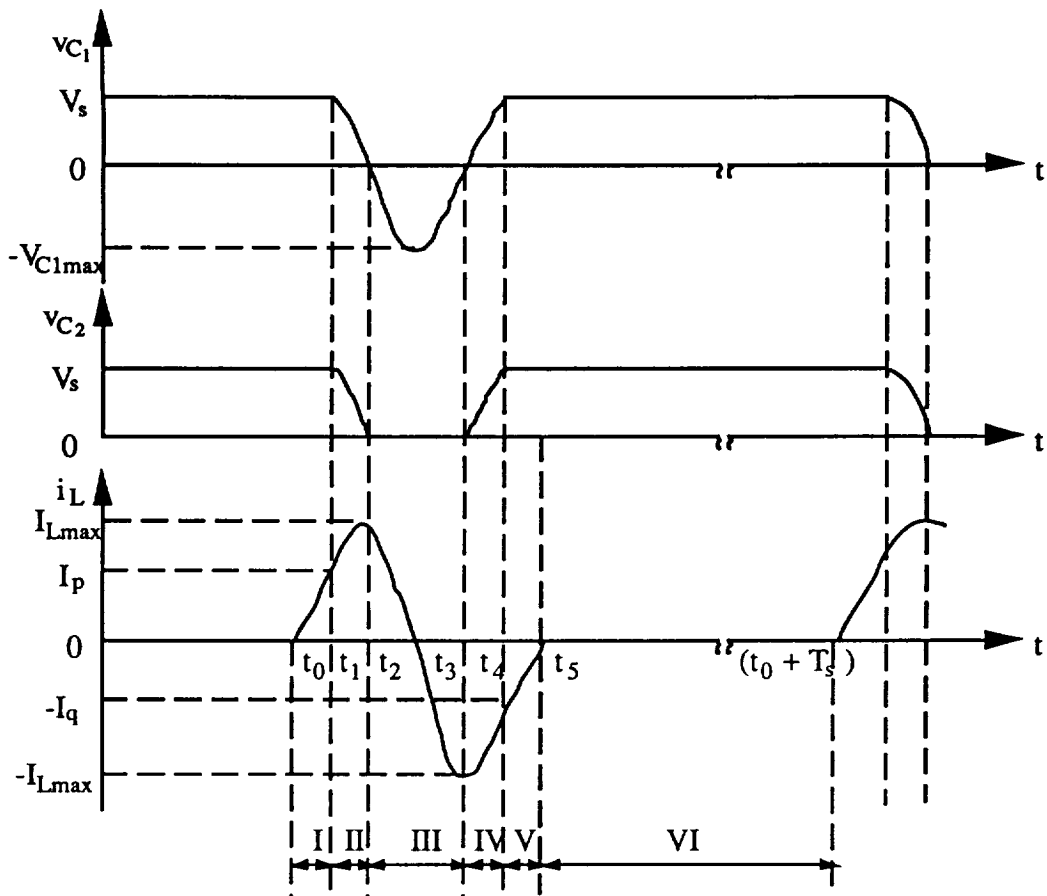


Figure 2. Waveforms for the ZVS PWM Inverter [1-3].

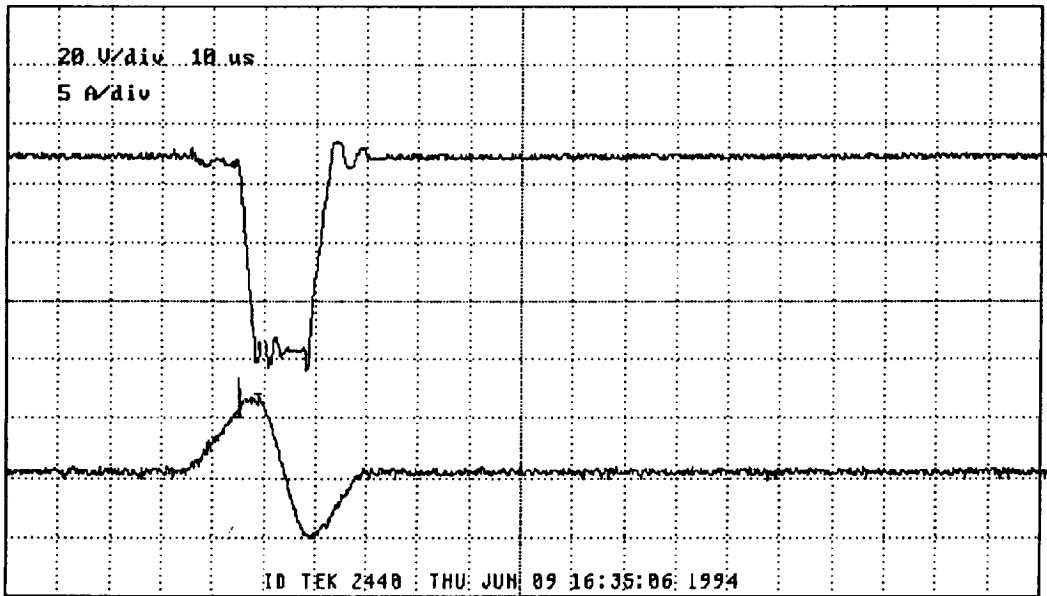


Figure 3. Inverter input voltage (top) and inductor current (bottom) versus time.

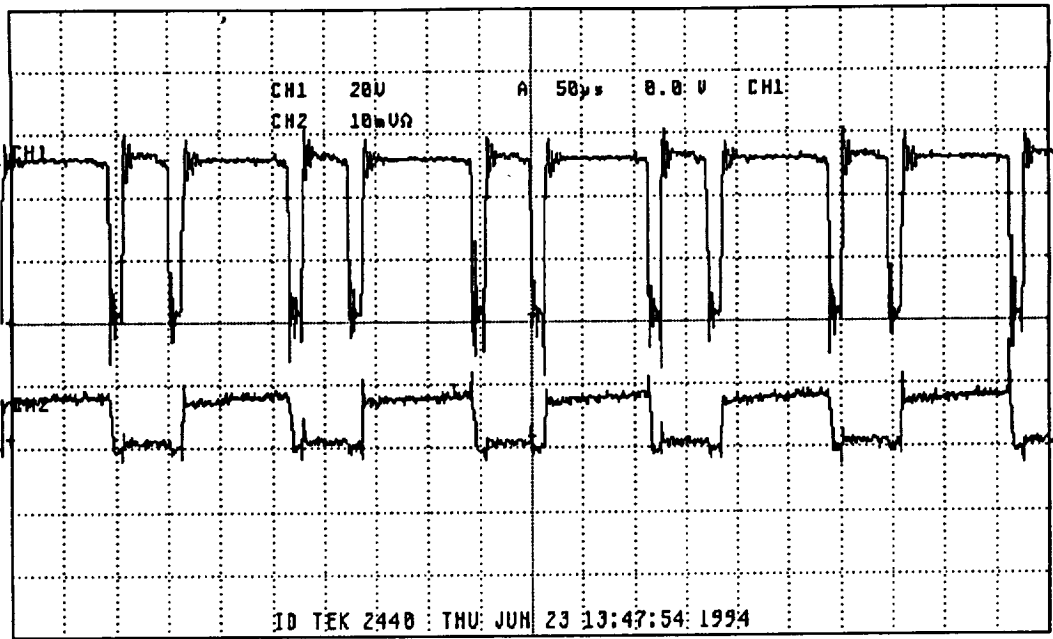


Figure 4. Inverter input voltage (top) and link current (bottom) versus time.